

# Operation of ILC250 at the Z-pole

Kaoru Yokoya, Kiyoshi Kubo, and Toshiyuki Okugi,  
High Energy Accelerator Research Organization (KEK), Japan  
Aug.27. 2019

ILC (International Linear Collider) is under consideration as the next global project of particle physics. Its Technical Design Report, published in 2013, describes the accelerator for the center-of-mass energies above 200GeV. The operation of ILC at lower center-of-mass energies has not been studied intensively. This report discusses the operation of the ILC at a center-of-mass 91.2GeV and presents a possible parameter set.

## 1 Introduction

When the serious design study of the ILC started in 2005, the first design criteria was “a continuous centre-of-mass energy range between 200 GeV and 500 GeV” (TDR[1], page 3). Hence, the TDR quoted the luminosities only for the center-of-mass energies at 200, 230, 250 GeV and above. Obviously, once ILC is built, lower energies such as Z-pole (91.2GeV) and W-pair threshold (160GeV) would be of interest, though these are not the main concern of ILC.

In the baseline design of ILC the positron production scheme using undulator magnets is adopted. In this scheme the electron beam, before going to the collision point, goes through undulators to produce photons (over several MeV) which create positrons on a target. To this end the electron energy must be at least about 125 GeV. For operation at  $E_{CM} \leq 250$  GeV TDR adopted the so-called 5+5Hz scheme<sup>1</sup>

The possibilities of ILC operation at the Z-pole (and W-pair threshold) was first discussed by N. Walker[2]. Later, K. Yokoya gave a short report at a workshop.[3]. These reports gave a possible luminosity range at the Z-pole by using a scaling law and pointed out many challenges to be studied later.

The luminosity is given by

$$\mathcal{L} = \frac{f_{rep} n_b N^2}{4\pi \sigma_x^* \sigma_y^*} H_D \quad (1)$$

where  $f_{rep}$  is the repetition rate of the beam pulse,  $n_b$  the number of bunches in a pulse,  $N$  the number of particles per bunch, and  $\sigma_{x(y)}^*$  is the horizontal (vertical) beam size at the IP (interaction point).  $H_D$  (luminosity enhancement factor) expresses the effects of the beam-beam force. With the optics around the IP fixed,  $\sigma_{x(y)}^*$  is proportional to the square root of the geometric emittance  $\varepsilon_{x(y)}$ . Since the geometric emittance is inversely proportional to the beam energy, a naive scaling expects  $\mathcal{L} \propto E_{CM}$ . However, the large geometric emittance at low energies causes a larger beam size at the final quadrupole magnets such that the beam halo may produce backgrounds to the experiments. Such halo particles usually are eliminated by collimators in upstream. However, too deep a collimation would cause further backgrounds and

---

<sup>1</sup>The electron linac is operated at 10Hz: 5Hz to accelerate the beam to  $\sim 150$  GeV which produces positrons and another 5Hz to accelerate the beam to  $E_{CM}/2$  for collision experiment. This is sometimes referred to as ‘10Hz’ operation. However, there is another 10Hz operation, in which all systems, the injectors, damping rings, main linacs etc., are operated at 10Hz to make 10Hz collisions. Thus, to distinguish from the latter we call the former ‘5+5Hz’.

enhancement of beam fluctuation by the wake field in the collimators. In such a case one has to relax the beta functions at the IP, which brings about a lower luminosity. If this happens in one of the  $x$  and  $y$  planes, then the luminosity would be proportional to  $E_{CM}^{3/2}$ , and if in both planes, to  $E_{CM}^2$ . The above report[2] gave a luminosity range  $1 - 1.5 \times 10^{33}/\text{cm}^2/\text{s}$ , corresponding to  $\mathcal{L} \propto E_{CM}^2$  or  $E_{CM}^{3/2}$  based on the luminosities at 200-250GeV in the TDR.

Table 1:

Proposed Parameters for Operation at Z-pole

The baseline parameters for 250GeV is listed for reference.

Center-of-Mass Energy	$E_{CM}$	91.2	250	GeV
Beam Energy	$E_{beam}$	45.6	125	GeV
Collision rate	$f_{col}$	3.7	5	Hz
Electron linac repetition rate		3.7+3.7	5	Hz
Pulse interval in electron main linac		135	200	ms
Electron energy for $e^+$ production		125	125	GeV
Number of bunches	$n_b$	1312	1312	
Bunch population	$N$	2	2	$\times 10^{10}$
Bunch separation	$\Delta t_b$	554	554	ns
RMS bunch length	$\sigma_z$	0.41	0.30	mm
Electron energy spread at IP (rms)	$\sigma_{E_-}/E_-$	0.30	0.188	%
Positron energy spread at IP (rms)	$\sigma_{E_+}/E_+$	0.30	0.150	%
Electron polarization	$P_-$	80	80	%
Positron polarization	$P_+$	30	30	%
Emittance from DR (x)	$\gamma\epsilon_x^{DR}$	4	4	$\mu\text{m}$
Emittance from DR (y)	$\gamma\epsilon_y^{DR}$	20	20	nm
Emittance at the linac exit (x)	$\gamma\epsilon_x^{IP}$	5	5	$\mu\text{m}$
Emittance at the linac exit (y)	$\gamma\epsilon_y^{IP}$	35	30	nm
Emittance at IP (x)	$\gamma\epsilon_x^{IP}$	6.2	5	$\mu\text{m}$
Emittance at IP (y)	$\gamma\epsilon_y^{IP}$	48.5	35	nm
Beta x at IP	$\beta_x^*$	18	13	mm
Beta y at IP	$\beta_y^*$	0.39	0.41	mm
Beam size at IP (x)	$\sigma_x^*$	1.12	0.515	$\mu\text{m}$
Beam size at IP (y)	$\sigma_y^*$	14.6	7.66	nm
Disruption Param (x)	$D_x$	0.41	0.51	
Disruption Param (y)	$D_y$	31.8	34.5	
Geometric luminosity	$\mathcal{L}_{geo}$	0.95	5.29	$10^{33}/\text{cm}^2/\text{s}$
Luminosity	$\mathcal{L}$	2.05	13.5	$10^{33}/\text{cm}^2/\text{s}$
Luminosity enhancement factor	$H_D$	2.16	2.55	
Luminosity at top 1%		99.0	74	%
Number of beamstrahlung	$n_\gamma$	0.841	1.91	
Beamstrahlung energy loss	$\delta_{BS}$	0.157	2.62	%

Since the above studies there have been several changes in the ILC design. Most relevant ones for our context are:

- The initial center-of-mass energy for the ILC was reduced from 500GeV to 250GeV in order to concentrate on the Higgs study.
- The undulator length was extended from 147m to 231m so that the electron beam of 125GeV can produce sufficient number of positrons. Thus, we do not need 5+5Hz scheme for  $E_{CM} = 250\text{GeV}$ .
- The normalized horizontal emittance at the IP was reduced from  $10\mu\text{m}$  to  $5\mu\text{m}$  by modifying the damping ring design. This change improved the luminosity at  $E_{CM} = 250\text{GeV}$  by a factor  $\sim 1.6$ . [5]

In the present report, taking into account these changes we give study results on the possible luminosity at the Z-pole.

Table 1 shows the preliminary parameter set to be described in this report. The study results for each item will be discussed in the later sections.

## 2 Repetition Rate

As mentioned in the introduction, the TDR adopted the ‘5+5Hz’ scheme for the operation at low energies. This scheme demands more electric power than the normal 5Hz operation but this is possible because the power system of 500GeV machine is available. For example, the electron linac would produce 45.6GeV and  $\sim 150\text{GeV}$  electron beams alternately. The sum of the power of these two is less than the power for 250GeV electron beam.

However, this is not true for the ILC 250GeV. The installed power is not sufficient for 5+5Hz operation. In this section we estimate the possible highest repetition rate under the limitation of the power system of ILC 250GeV.

First, let us discuss how to switch the beam energy. To get a 45.6GeV electron beam with a 125GeV linac, one might want to accelerate the beam to 45.6GeV with the full gradient and turn off the power for the rest of the linac. This is better from the view point of the beam dynamics in the powered cavities. However, for avoiding the effects of the beam-induced field in the un-powered part of the linac, one has to detune the cavities quickly (a few Hz). This can only be done by piezo tuners but the dynamic range of the equipped tuners is far from this requirement. Thus we have to accelerate the electron beam uniformly over  $\sim 5\text{km}$  with a very low gradient (8.76MV/m compared with 31.5MV/m for 125GeV) <sup>2</sup> Thus, the electron linac must be operated with gradients 31.5MV/m and 8.76MV/m, alternately.

The possible parameters of the RF system are shown in Table 2. (This estimation was done by T. Matsumoto.[4]). The parameters of the normal operation for  $E_{CM} = 250\text{GeV}$  are identical to the one in the left column except the repetition is 5Hz. Since the gradient is low for the 45.6GeV beam, the klystron power is low and the fill time (and hence the RF pulse length) is short. One can find from this table that the integral of the modulator output in one cycle is  $14.66\text{MW} \times 1.65\text{ms} + 7.83\text{MW} \times 1.06\text{ms} = 32.5\text{kJ}$ , which is larger than the first term (125GeV) by a factor 1.34. Therefore, the highest possible repetition rate is  $5\text{Hz}/1.34 \approx 3.7\text{Hz}$ . There will be some margin in the actually installed power which can raise the rate a little, but we adopt 3.7+3.7Hz operation in the following.

---

<sup>2</sup> $31.5 \times (45.6 - 15) / (125 - 15) = 8.76\text{ MV/m}$ , since the injection energy to the main linac is 15GeV.

Table 2: RF system parameters for alternating operation of 125GeV and 45.6GeV

	e <sup>+</sup> production	collision	
Final beam energy	125	45.6	GeV
Average accelerating gradient	31.5	8.76	MV/m
Peak power per cavity	189	77.2	kW
Klystron peak power	9.82	4.15	MW
Klystron efficiency	67	53	%
Modulator output	14.66	7.83	MW
Fill time	0.927	0.328	ms
Beam pulse length	0.727	0.727	ms
RF pulse length	1.65	1.06	ms
Repetition rate	3.7	3.7	Hz

### 3 Damping Rings

Basically, the damping rings designed for the TDR are capable of 5+5Hz operation by a reinforcement of the wiggler magnets and the RF system. However, the design has been changed slightly since AWLC2017 at SLAC[5] (smaller horizontal emittance  $6\mu\text{m}$  to  $4\mu\text{m}$ ). It must be checked whether the new design accepts 3.7+3.7Hz operation.

In 3.7+3.7Hz operation, the beam stay in the damping ring for  $1/3.7\text{Hz}/2=135\text{ms}$ , while 200ms in the baseline 5Hz operation.

Figure.1 shows the transverse damping time as a function of the wiggler strength parameter. Factor 1 corresponds to the field 1.29T (curvature  $0.07745\text{m}^{-1}$ ).

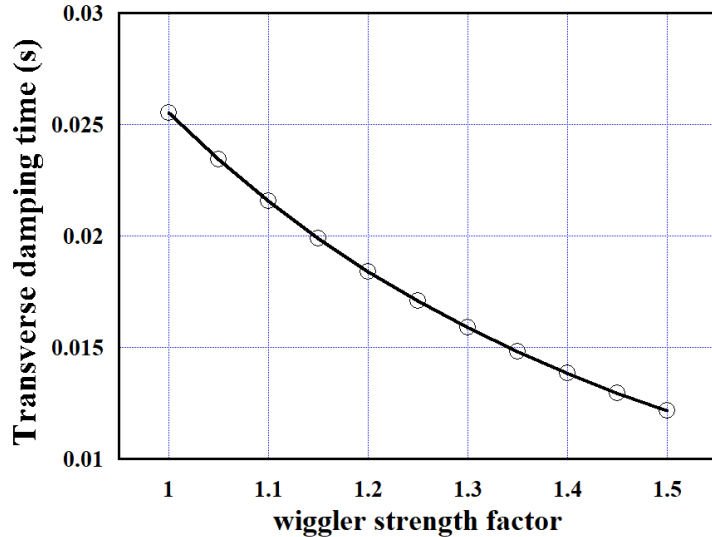


Figure 1: The transverse damping time as a function of the wiggler strength parameter.

Figure.2 shows the equilibrium and extracted emittances from the damping ring as functions of the wiggler strength parameter. The initial emittance is  $1 \times 10^{-3}$  rad·m (for positron). As the vertical-horizontal coupling, 0.005 is assumed.

The figure on the right shows that the extracted vertical beam emittance is too large if the wiggler strength factor  $\lesssim 1.1$  because the damping is not fast enough. The strength factor  $\sim 1.15$  ( $B = 1.48$  Tesla) gives  $\gamma\epsilon_x \approx 4\mu\text{m}$   $\gamma\epsilon_y \approx 21\text{nm}$ . The latter is slightly larger than the value in Table 1 (20nm) but a slight improvement of the coupling would be sufficient.

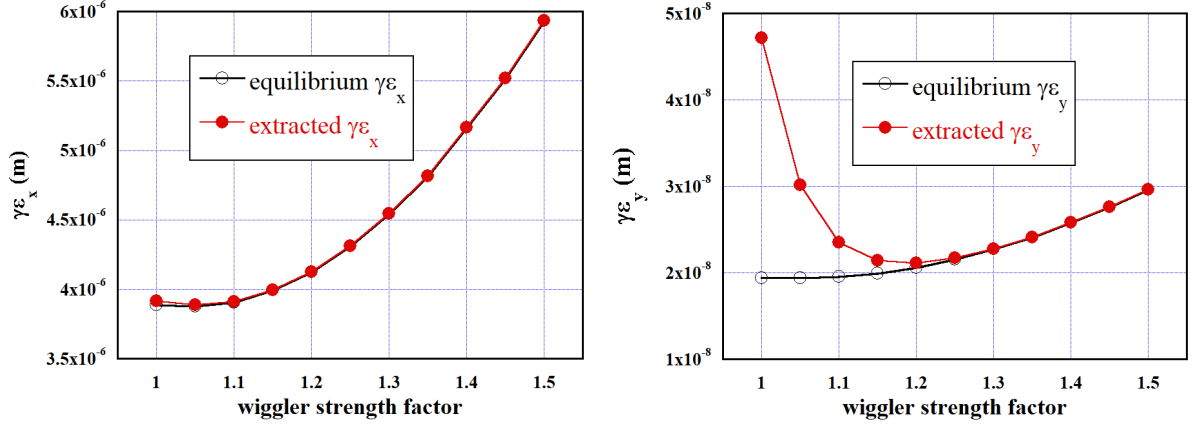


Figure 2: Horizontal (left) and vertical (right) normalized emittance as functions of the wiggler field strength. The open circles are the equilibrium emittance and the solid (red) circles are the emittance when extracted at 135ms after injection. 0.005 is assumed as the vertical-horizontal coupling. The effects of the intra-beam scattering is included.

Because the wiggler strength is increased, the dynamic aperture of the damping rings must be re-examined. The requirements are, as in TDR:

- Normalized betatron amplitude  $A_x + A_y \leq 0.07\text{m} \cdot \text{rad}$
- Energy deviation  $\leq 0.75\%$

The wiggler strength factor is set to 1.15 (curvature  $0.0891 \text{ m}^{-1}$ ). The acceptance criterion is the survival after 1000 turns.

Figure.3 show the results. The plot on the left (right) shows the aperture without (with) the sextupole components of the wiggler field. (Adopted sextupole field is  $(\Delta B/B) = 0.066$  at  $x = 10\text{mm}$  as in TDR[1] page 115.) The half circle at the center-bottom shows the required aperture for the transverse emittance mentioned above. As is seen, the dynamic aperture is sufficient. The sextupole field has no significant effects. The magnet error has not been included here, but its effect was not significant in the previous calculation with the wiggler strength 1[3].

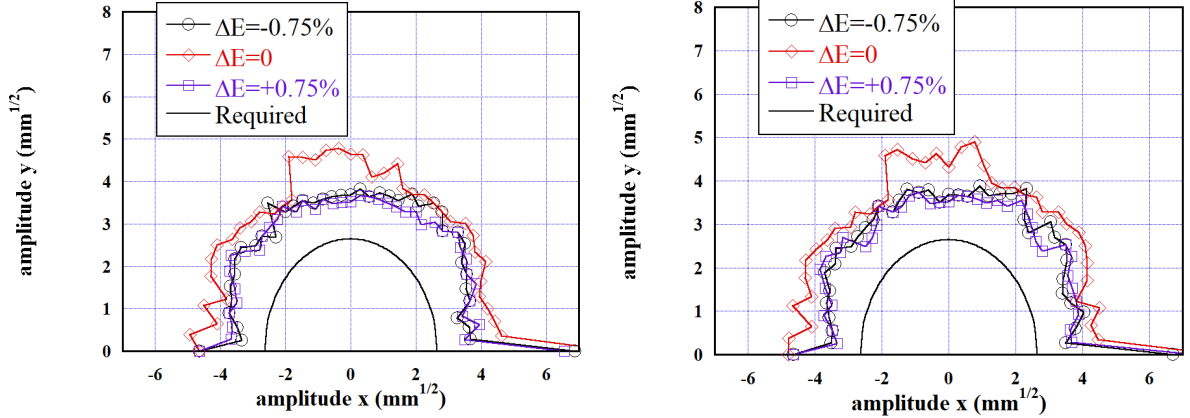


Figure 3: Dynamic aperture of the damping rings with increased wiggler strength. The plot on the left (right) is the case without (with) the sextupole components of the wiggler field.

All simulations in this section were done using the computer code SAD[6].

## 4 Electron Main Linac

There are several issues to be studied on the 3.7+3.7Hz operation of the electron main linac.

- (a) The RF system must deliver different pulses (power and pulse length) alternatingly with an interval of 135ms.
- (b) The orbits for the 45.6GeV (colliding) and 125GeV (positron production) beams are different even without alignment errors due to the earth's curvature. This difference must be corrected before injection to the undulator section.
- (c) The emittance increase by the misalignment must be checked. In particular the major concern is the colliding beam because the accelerating gradient is very low.

As mentioned in the Sec.2, the 45.6GeV (colliding) beam must be created by uniform acceleration over the entire linac rather than full gradient followed by detuned cavities. There seems to be no other RF-technical problem of (a) in the alternating operation.

A simulation was done for the issue (b). Figure.4 shows the orbit difference. It amounts to  $\sim 1\text{cm}$  at the end of the linac. This difference (and the orbit angle difference, which is not shown here) must be corrected before entering the undulator section by using 3.7Hz pulsed magnets. A short section must be allocated (the required length still need to be estimated) but there is no problem as far as the field strength is concerned. It must be checked whether the field can be accurate enough. In this respect it is better to bend the positron production beam, though the energy is higher, because the colliding beam must be extremely stable in particular in the vertical plane.

In addition, the wakefield effects (mainly resistive wall) for the colliding beam in the undulator section should be studied in more detail because the beam energy is low. If the effect turns out to be serious, we have to prepare a beamline to bypass the undulator.

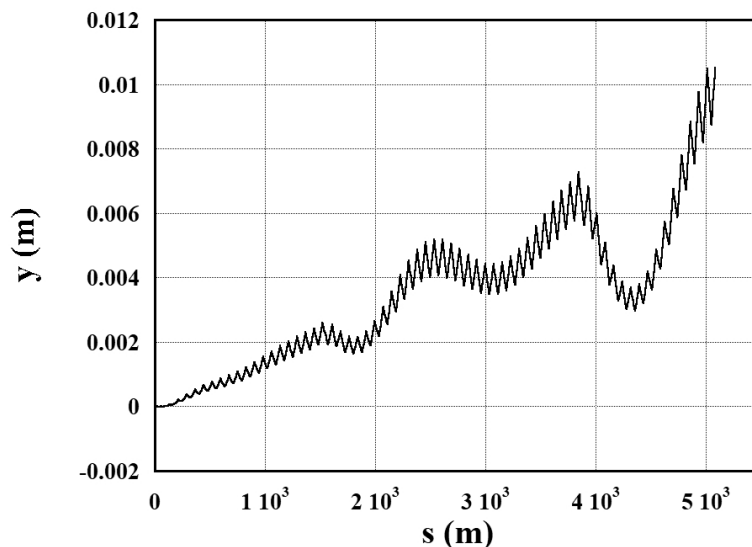


Figure 4: The vertical orbit difference between 45.6 and 125GeV beams as a function of the length  $s$  along the linac. No errors included.

For the issue (c) simulations have been done under the following assumptions.

- The vertically curved orbit as mentioned above.
- Orbit correction was done for the colliding beam (45.6GeV). The same steering setting was used for the positron production beam since the emittance increase is not an issue for the latter.
- The assumed misalignments (every cavity and quadrupole magnet are misaligned independently, ignoring the module structure.)
  - Quadrupole magnets offset 0.36mm
  - Cavity offset 0.67m, tilt 0.3mrad
  - BPM offset  $1\mu\text{m}$

The numbers are r.m.s of Gaussian distribution cut at 3 sigmas.

- Initial normalized emittance  $\gamma\epsilon_y=20\text{nm}$
- DFS (Dispersion-free steering) with energy change 20%.

Two cases were simulated for the bunch length and the initial energy spread:

- Bunch length 0.3mm, energy spread 1.2%
- Bunch length 0.41mm, energy spread 0.9%

The reason of the second case is mentioned in the next section. In the case of longer bunches the expected emittance increase due to the wake field (combined with misalignment) is larger but that due to the energy spread is smaller.

Figure.5 shows the vertical emittance increase in the misaligned linac as a function of the final beam energy. What is shown is the average emittance increase of 100 different random number sets.<sup>3</sup>

The average emittance increase of the 45.6GeV beams with  $\sigma_z = 0.41\text{mm}$  is 6.3nm, sufficiently smaller than the emittance budget 10nm. (Note that the emittance increase would amount to  $\sim 16\text{nm}$  for Z-pole operation of ILC500[3] due to the even lower gradient in longer  $\sim 10\text{km}$  linac.) The increase in the shorter bunch case is slightly smaller, which indicates the effect of the wake is slightly larger than that of the energy spread.

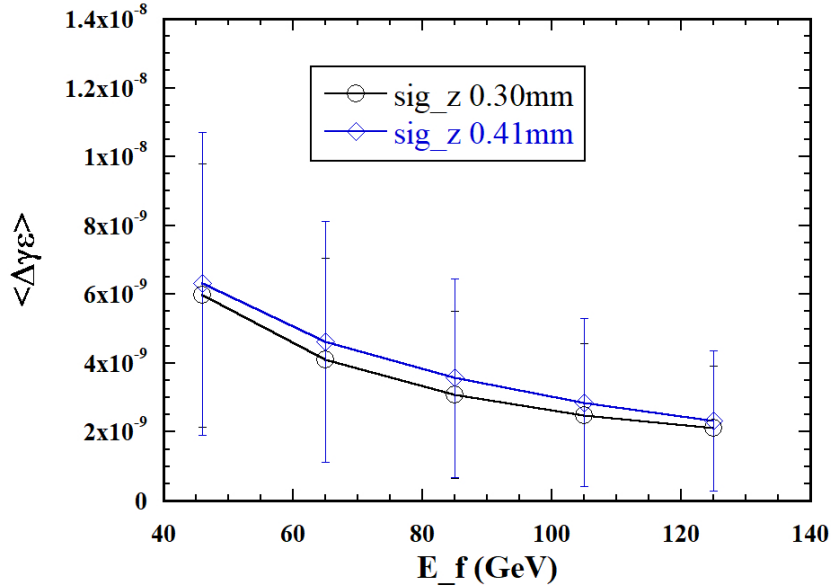


Figure 5: The vertical emittance increase in the main linacs as a function of the final beam energy. Two cases of different  $\sigma_z$  are shown. The error bars indicate one standard deviation in 100 runs with different random number seeds.

<sup>3</sup>Note:  $E_f=125\text{GeV}$  in this table indicates the case where the orbit tuning is done for this energy. This is true for the baseline case  $E_{CM}=250\text{GeV}$ . However, the 125GeV beam for the positron production in 3.7+3.7Hz operation is different because the tuning is done for 45.6GeV beam. The emittance of the positron production beam will be significantly larger. Nonetheless, this is not an issue because the positron production does not require a very low emittance beam.



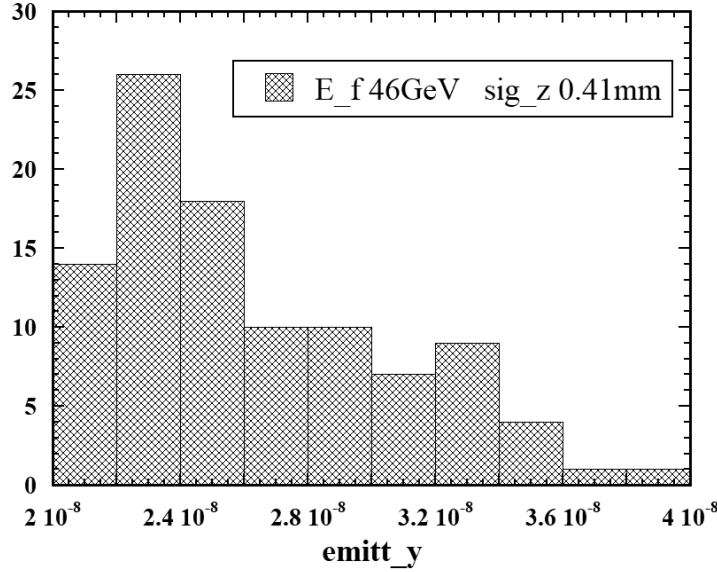


Figure 6: Distribution of the vertical emittance at the linac end over 100 different random number seeds. Final beam energy 45.6GeV.  $\sigma_z = 0.41\text{mm}$ .

Figure.6 shows the distribution of the final emittance for the case of the final beam energy 45.6GeV and  $\sigma_z = 0.41\text{mm}$ . The final emittance at the 90% confidence level is  $\gamma\epsilon_y \sim 33\text{nm}$ , which slightly exceeds the budget but still in an acceptable level.

## 5 Beam Delivery System (BDS)

There are three major issues in BDS related to the Z-pole operation.

- Collimation depth as explained in the introduction
- Momentum band width
- Wake field effects

### Collimation Depth

The geometric emittance is inversely proportional to the beam energy. It is a factor  $125/45.6=2.74$  times larger than at  $E_{CM}=250\text{GeV}$ . The synchrotron radiation from particles in the halo with large angles at the IP cause background to the experiment. These particles should be eliminated by collimators upstream. However, the required collimation in the horizontal plane is too deep ( $\sim 6\sigma_x$ ) with the TDR parameters even at  $E_{beam} = 125\text{GeV}$  ( $E_{CM}=250\text{GeV}$ ). This was the reason that we adopted a smaller horizontal emittance  $\gamma\epsilon_x = 10\mu\text{m} \rightarrow 5\mu\text{m}$  by improving the damping ring design since 2017[5]. Now, this problem is more serious at the Z-pole. Since the angle at the IP is proportional to  $1/\beta^*$ , to keep the collimation depth  $\sim 6\sigma_x$ , the horizontal beta function should be

$$\beta_x^* \gtrsim 13\text{mm}/2.74 \times (10/5) = \sim 18\text{mm} \quad (2)$$

where 13mm is the TDR value at  $E_{CM}=250\text{GeV}$ .

On the other hand there is no problem in the collimation depth in the vertical plane because it has a large margin ( $\sim 40\sigma_y$ ) at  $E_{CM}=250\text{GeV}$ .

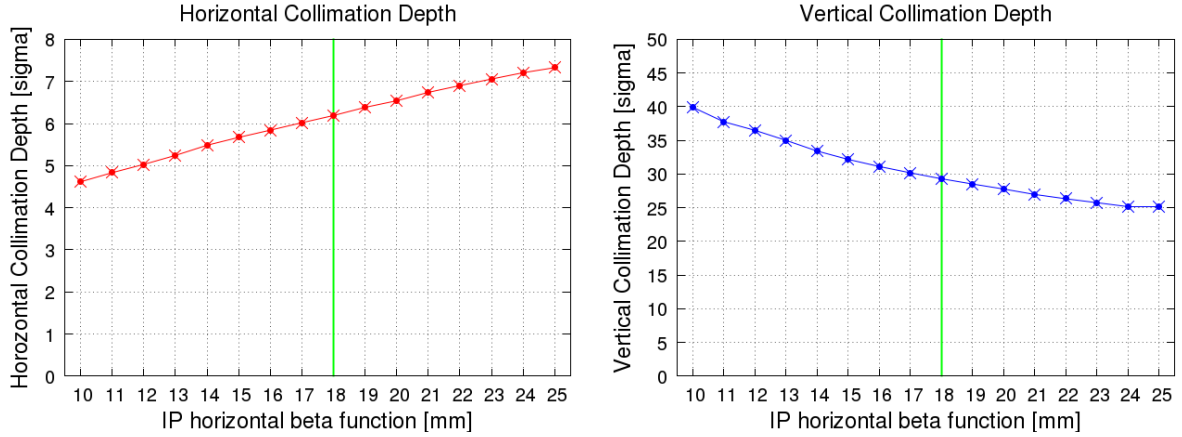


Figure 7: Collimation depth as a function of the horizontal beta function. The left(right)-hand-side is the depth in the horizontal (vertical) plane. The same beam pipe aperture is used as in ILC 250GeV.  $\beta_x^* \times \beta_y^*$  is fixed.

Figure 7 shows the collimation depth obtained by simulation. As is seen, the collimation depth in the horizontal plane is  $\geq 6\sigma_x$  with  $\beta_x^* = 18\text{mm}$ , which confirms eq.2.

### Momentum Band Width

The relative beam energy spread  $\sigma_E/E$  at the IP is proportional to  $1/(E\sigma_z)$ . It is  $\sim 0.15\%$  at  $E_{CM}=250\text{GeV}$ <sup>4</sup> If the bunch length (0.3mm) is fixed, the energy spread for Z-pole operation is  $\sim 0.41\%$ . This large (relative) energy spread may cause an emittance growth in the BDS due to the chromatic effects.

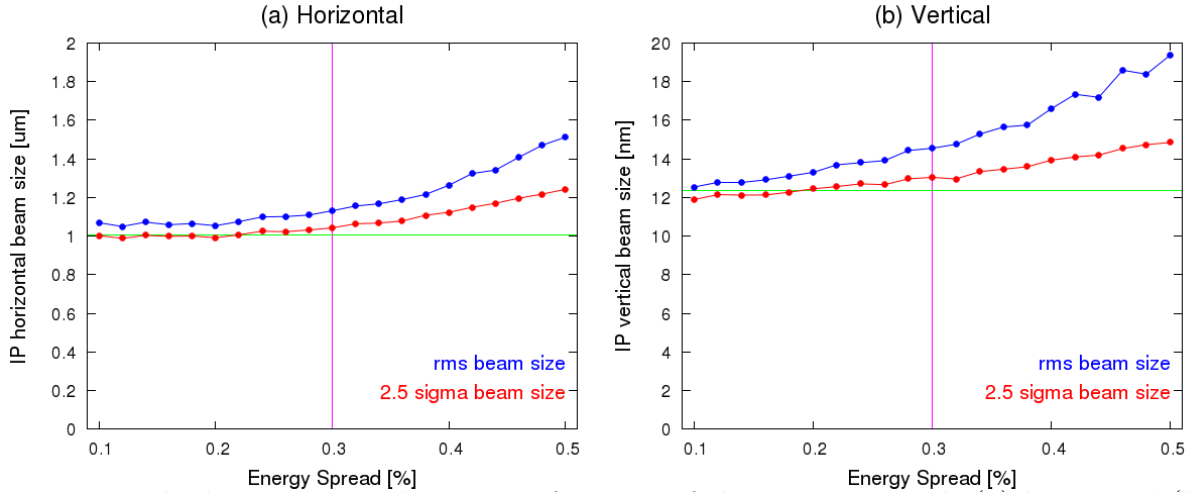


Figure 8: The beam size at the IP as a function of the energy spread. (a) horizontal (b) vertical. The blue spots show the r.m.s. of the whole beam size and the red spots show the r.m.s.=size with  $> 2.5\sigma$  tail cut off.

Figure 8 shows the beam sizes as functions of the energy spread. Here, the magnet errors are not included. This plot shows the beam size growth is too large if the energy spread is 0.41%.

<sup>4</sup>This is the positron energy spread quoted in the TDR. The electron energy spread is larger ( $\sim 0.19\%$ ) because of the increase in the undulator section. Here we use the value for positron for the scaling base because the undulator effect is tiny at 45.6GeV.

To reduce the energy spread, we adopt a longer bunch length in the bunch compressor  $0.3 \rightarrow 0.41\text{mm}$ , which will bring about a smaller energy spread  $\sigma_E/E = 0.41\% \rightarrow 0.3\%$  at the IP. The beam sizes at IP ( $2.5\sigma$ ) in such a case are  $\sim 1.04\mu\text{m}$  (horizontal) and  $\sim 12.7\text{nm}$  (vertical) in the absense of magnet errors and wakefields from Figure 8.

This long bunch has two side effects.

First, the transverse wake field in the main linac and the BDS increases by the factor  $0.41/0.3$ . The previous section showed that the emittance increase in the main linac due to this reason is acceptable.

Another side effect is the increased disruption parameter at the IP. This will be mentioned in the next section.

### **Tuning of the BDS with magnet errors and wakefield**

Simulations including the magnet errors and the process of beamline tuning were done, assuming the errors listed in Table 3.

Table 3: Magnet errors used in the simulation of BDS

Bend	rotation	100 $\mu\text{rad}$
	field strength ( $\Delta\rho/\rho$ )	$1 \times 10^{-4}$
	bend-to-BPM alignment	100 $\mu\text{m}$
Quad	alignment ( $x,y$ )	100 $\mu\text{m}$
	rotation	100 $\mu\text{rad}$
	field strength ( $\Delta K_1/K_1$ )	$1 \times 10^{-4}$
	sextupole component ( $B_2/B_1$ at $r=1\text{cm}$ )	$1 \times 10^{-4}$
	quad-to-BPM alignment	5 $\mu\text{m}$
Sextupole	alignment ( $x,y$ )	100 $\mu\text{m}$
	rotation	100 $\mu\text{rad}$
	field strength ( $\Delta K_2/K_2$ )	$1 \times 10^{-4}$
	sext-to-BPM alignment	5 $\mu\text{m}$

Figure 9 shows a example of the tuning process in the presense of magnet errors (but no wake fields). It shows the vertical beam size vs. number of tuning knobs. Two cases of different r.m.s. errors of the distance from the BPM center to the quadrupole/sextupole field center ( $5\mu\text{m}$  and  $10\mu\text{m}$ ) are shown.  $10\mu\text{m}$  is the value used in the BDS simulations of ILC so far. Improvement to  $\sim 5\mu\text{m}$  during a few years of operation experience will be possible.

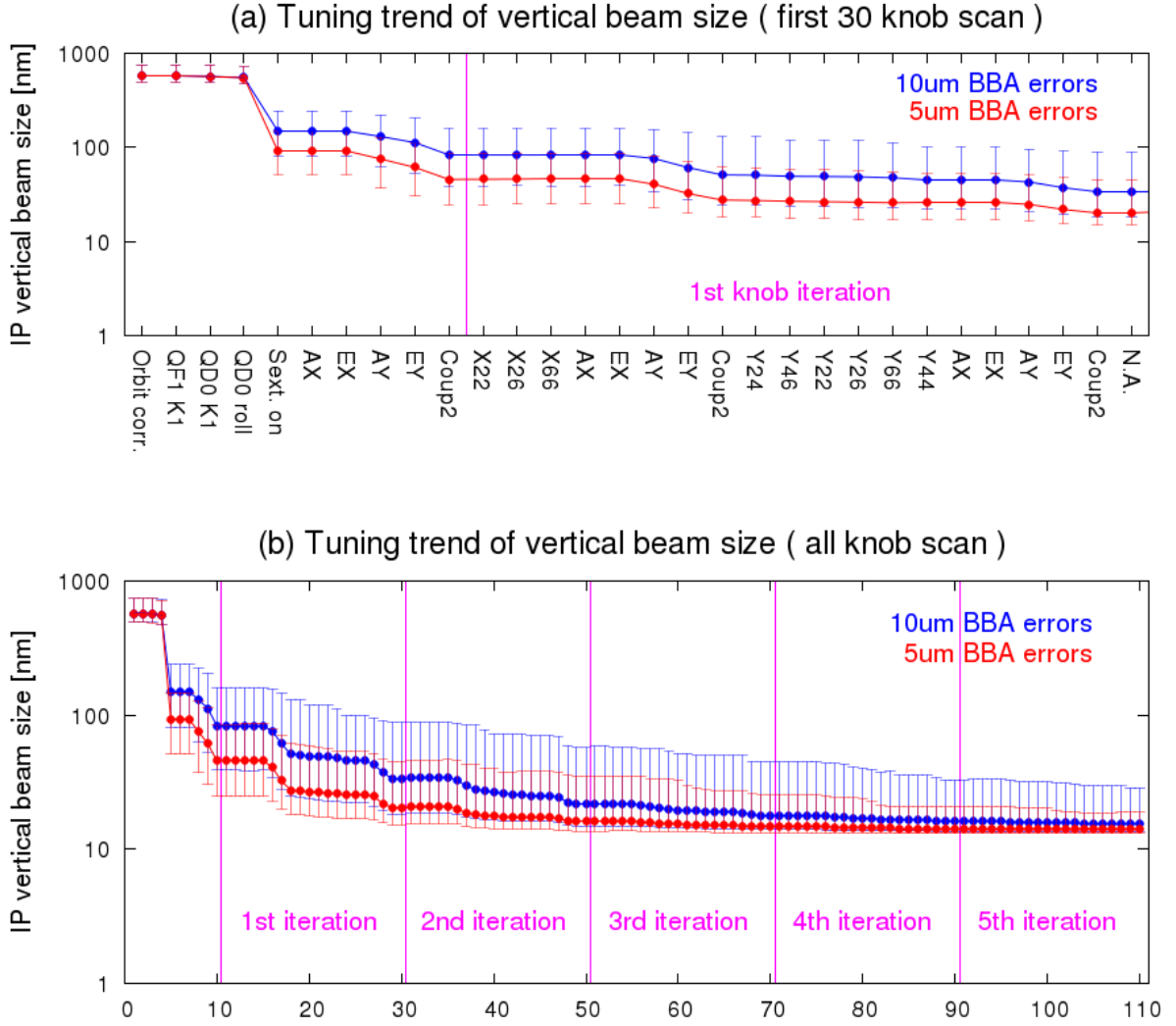


Figure 9: Vertical beam size vs. number of knob scans in the process of BDS tuning. (a) shows the first 30 knobs. (b) shows all knobs.

Table 4 shows the beam sizes obtained in this way. These values are averages of 100 random number seeds. The case with magnet errors and tuning is shown in the row (2).

Table 4:  
Simulation results of the vertical beam sizes.  
The offset  $300\mu\text{m}$  of the wake sources is used for the row (3) and (4).

	$\sigma_x^*$ ( $\mu\text{m}$ )	$\sigma_y^*$ (nm)
(1) No errors	1.04	12.7
(2) Magnet errors and correction	1.12	14.0
(3) Magnet errors + static wake + correction		14.3
(4) Magnet errors + static&dynamic wake + correction		14.6

Since the beam energy is very low at the Z-pole compared with the baseline energy  $E_{CM} = 250\text{GeV}$  and, moreover, we adopted the longer bunch, the effects of the transverse wake are expected to be significant.

The most important wake sources are the 107 BPMs (Beam Position Monitor) distributed over the BDS beamline. They are associated with bellows, and flange gaps. We assumed the wake sources are dislocated by  $300\mu\text{m}$  in the simulations.

The correction of the wake effects is done by adding artificial wake sources mounted on movers and by changing their position so as to cancel the wake effects. This is done only in the vertical plane since the effects on the horizontal plane is minor. The row (3) in Table 4 the result with static wake effects and tuning. In this simulation we assumed that the wakefields by bellows and flange gaps are minimized by using RF contacts. If not, the resulting beam size would be  $\sim 15.8\text{nm}$  instead of  $14.3\text{nm}$ .

In addition to the static wakefield effects described above, there is a ‘dynamic effects’ coming from the beam jitter from upstream. Since many wake sources are placed where  $\beta$  is large and the phase advance from the IP is  $\pi/2$ , the beam jitter can be enhanced by the wakefields. It is compensated for by the fast feedback system developed for the ILC. From our experience we assumed the feedback system can suppress the beam angle jitter to 10%.

The row (4) in Table 4 shows the vertical beam size in the presense of the static/dynamic wake effects and the correction. The resulting vertical beam size was  $14.6\text{nm}$ . This is adopted in Table 1.

These simulations show that the following issues are important for the BDS tuning especially at the Z-pole.

- Accurate alignment between the magnet field centers and the electric center of BPMs.
- Sufficient RF contact for the bellows and flange gaps to minimize the wakes.
- Relaxing the intensity dependence due to the static wake effects by wakefield knobs.

## 6 Beam-Beam Interaction

Figure.10 shows the luminosity spectrum with the parameters listed in Table 1. The dashed curve shows the initial distribution normalized at the peak. As is seen, the contibution of the beamtrahlung is very small.

Because of the longer bunch to reduce the energy spread, the vertical disruption parameter is slightly enlarged ( $D_y = 31.8$ ). Nonetheless, it is still lower than the value 34.5 for  $E_{CM} = 125\text{GeV}$  case. Therefore, the tolerance of the beam offset will not be severer ( $0.1\sigma_y^*$ ).

## 7 Luminosity Upgrade

In the present design the major limitation of the luminosity comes from the energy band-width of the final focus system and the large vertical disruption parameter.

The former may be a little improved by adopting a shorter final quadrupole magnet. In fact the TDR adopted 2m long magnet which was split into two 1m magnets. Both are excited for  $E_{CM} = 500\text{GeV}$  but the upstream one is turned off for low energy operations. This helps in increasing the horizontal collimation depth from  $\sim 5\sigma_x$  to  $\sim 6\sigma_x$  at  $E_{CM} = 250\text{GeV}$ . However, we cannot expect a large improvement of the collimation depth at the Z-pole operation by a further reduction of the magnet length, say, to 50cm.

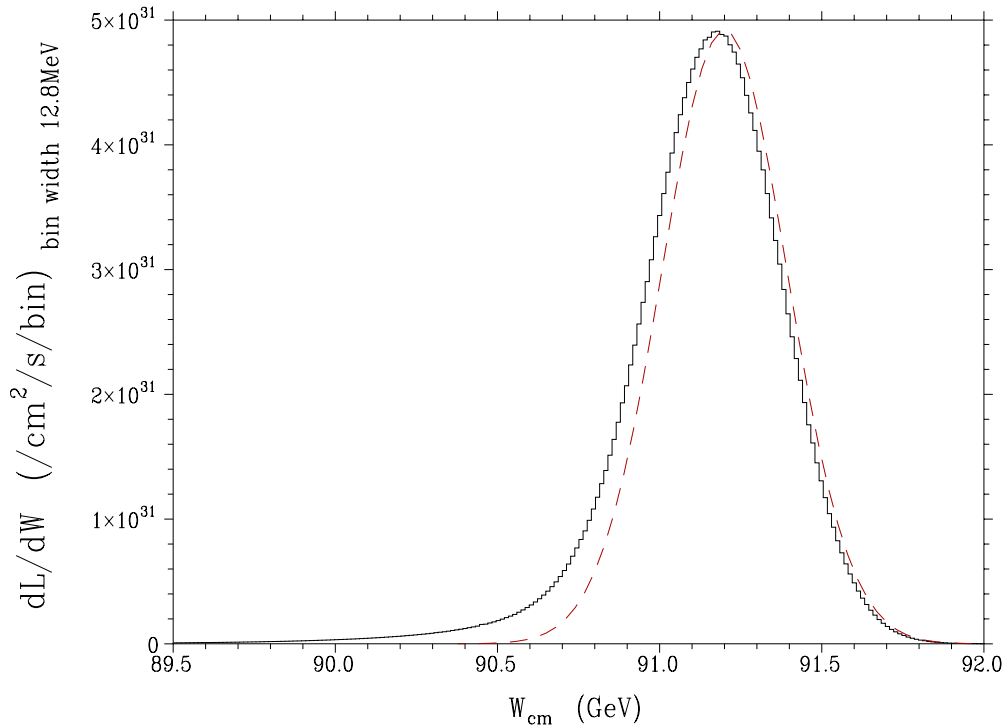


Figure 10: Luminosity spectrum. The red dashed curve shows the initial distribution normalized at the peak.

The latter is an issue of the beam position control at the IP. Since the beamstrahlung is negligible at Z-pole, one can further reduce the horizontal beam size in this respect, if an even larger disruption parameter is acceptable. The adoption of the so-called traveling focusing might allow a larger disruption but this is beyond the scope of this note.

On the other hand we do not foresee a major obstacle in doubling the luminosity by doubling the number of bunches from 1312 to 2625. Once the RF system is reinforced for doubled bunches, we expect to reach  $\mathcal{L} \sim 4.2 \times 10^{33}/\text{cm}^2/\text{s}$  at Z-pole.

When ILC is extended to 500GeV, there will be a chance to adopt the scheme proposed in [2], where the 250GeV electron main linac is split into two parts, upstream part ( $> 80\text{GeV}$  for W-pair) for the colliding beam and the downstream part ( $> 125\text{GeV}$  with an additional electron gun) for positron production. If this possibility is to be taken into account later, some preparation is necessary for the first construction (e.g., a space for the transport line of the colliding beam).

## 8 Summary

We estimated the luminosity of ILC for 250GeV at the center-of-mass energy for Z-pole. In addition to the change of the horizontal emittance, which has already been announced for maximizing the luminosity at 250GeV, we made the following changes of the parameters:

- Reduced the repetition rate from 5+5Hz to 3.7+3.7Hz because of the limited power consumption of the electron linac.

- Increased the bunch length from 0.3mm in TDR to 0.41mm in order to reduce the beam energy spread for relaxing the issue of the momentum bandwidth of the final focus system.
- Increased the  $\beta_x^*$  from 13mm for  $E_{CM} = 250\text{GeV}$  to 18mm for relaxing the requirement of the horizontal collimation.

The resulting luminosity is  $2.1 \times 10^{33}/\text{cm}^2/\text{s}$ , which is significantly higher than the value ( $\sim 1.5 \times 10^{33}$ ) from the previous simple scaling in spite of the reduced repetition rate.  $\propto E^{1.5}$  from 250GeV in TDR.

It is presumably possible to double the luminosity when the doubled bunch option (2625 bunches) of ILC is realized.

## References

- [1] The International Linear Collider, Technical Design Report volume 3.II: Accelerator Baseline Design. 2013.  
<https://www.linearcollider.org/ILC/Publications/Technical-Design-Report>
- [2] “ILC possibilities at Z and W”, N. Walker,  
<http://ilcdoc.linearcollider.org/record/63004?ln=ja>
- [3] “Z-pole Operation”, LCWS2016 at Morioka,  
<https://agenda.linearcollider.org/event/7371/contributions/38173/>
- [4] Toshihiro Matsumoto, KEK. Private communication.
- [5] “Overview of ILC optimization at the center of mass energy of 250GeV”, K. Yokoya, AWLC2017, June 28, 2017.  
<https://agenda.linearcollider.org/event/7507/timetable/#20170628.detailed>,  
“Preliminary study for lower horizontal emittance”, K. Kubo, AWLC2017, June 29, 2017.  
<https://agenda.linearcollider.org/event/7507/timetable/#20170629.detailed>
- [6] SAD is a computer program for accelerator design;  
<http://acc-physics.kek.jp/SAD/index.html>